

RESEARCH

Open Access



# Effect of strontium on transcription factors identified by transcriptome analyses of bovine ruminal epithelial cells

Panpan Tan<sup>1</sup>, Yazhou Wang<sup>1</sup>, Linshan Mei<sup>1</sup>, Juan J. Loor<sup>2</sup>, Chenxu Zhao<sup>1</sup>, Yezi Kong<sup>1</sup>, Fangyuan Zeng<sup>1</sup>, Baoyu Zhao<sup>1\*</sup> and Jianguo Wang<sup>1\*</sup>

## Abstract

**Background** Strontium (Sr) has similar physicochemical properties as calcium (Ca) and is often used to evaluate the absorption of this mineral. Because the major route of Ca absorption in the bovine occurs in the rumen, it is essential to understand whether Sr impacts the ruminal epithelial cells and to what extent.

**Results** In the present study, RNA sequencing and assembled transcriptome assembly were used to identify transcription factors (TFs), screening and bioinformatics analysis in bovine ruminal epithelial cells treated with Sr. A total of 1405 TFs were identified and classified into 64 families based on an alignment of conserved domains. A total of 174 differently expressed TFs (DE-TFs) were increased and 52 DE-TFs were decreased; the biological process-epithelial cell differentiation was inhibited according to the GSEA-GO analysis of TFs; The GO analysis of DE-TFs was enriched in the DNA binding. Protein-protein interaction network (PPI) found 12 hubs, including *SMAD4*, *SMAD2*, *SMAD3*, *SP1*, *GATA2*, *NR3C1*, *PPARG*, *FOXO1*, *MEF2A*, *NCOA2*, *LEF1*, and *ETS1*, which verified genes expression levels by real-time PCR.

**Conclusions** In this study, *SMAD2*, *PPARG*, *LEF1*, *ETS1*, *GATA2*, *MEF2A*, and *NCOA2* are potential candidates that could be targeted by Sr to mediate cell proliferation and differentiation, as well as lipid metabolism. Hence, these results enhance the comprehension of Sr in the regulation of transcription factors and provide new insight into the study of Sr biological function in ruminant animals.

**Keywords** Strontium, Transcription factors, Cell differentiation, Lipid metabolism

\*Correspondence:

Baoyu Zhao  
zhaobaoyu12005@nwsuaf.edu.cn  
Jianguo Wang  
jgwang0625@nwsuaf.edu.cn

<sup>1</sup>College of Veterinary Medicine, Northwest A&F University, Yangling 712100, Shaanxi, China

<sup>2</sup>Department of Animal Sciences, Division of Nutritional Sciences, University of Illinois, Urbana, IL 61801, USA



© The Author(s) 2024. **Open Access** This article is licensed under a Creative Commons Attribution 4.0 International License, which permits use, sharing, adaptation, distribution and reproduction in any medium or format, as long as you give appropriate credit to the original author(s) and the source, provide a link to the Creative Commons licence, and indicate if changes were made. The images or other third party material in this article are included in the article's Creative Commons licence, unless indicated otherwise in a credit line to the material. If material is not included in the article's Creative Commons licence and your intended use is not permitted by statutory regulation or exceeds the permitted use, you will need to obtain permission directly from the copyright holder. To view a copy of this licence, visit <http://creativecommons.org/licenses/by/4.0/>. The Creative Commons Public Domain Dedication waiver (<http://creativecommons.org/publicdomain/zero/1.0/>) applies to the data made available in this article, unless otherwise stated in a credit line to the data.

## Background

Strontium (Sr) is a Group II alkaline-earth metal with similar physicochemical properties to calcium (Ca). As a bone-seeking element, Sr has dual effects in regulating bone metabolism, on the one hand, Sr promotes bone formation by stimulating osteoblasts, and on the other hand, Sr suppresses bone resorption by inhibiting osteoclasts, resulting in increased bone deposition rates and bone mineral density [1, 2]. It has been widely used to treat osteoporosis in the form of Sr ranelate to promote osteogenic proliferation and differentiation via various pathways [3–6]. In primary bovine chondrocytes, Sr promotes proliferation and inhibits differentiation via the TGFβ/SMAD pathway [7]. In sheep and dairy cows, Sr concentration in the blood plasma can serve as an index of ruminal Ca absorption capacity under different states of Ca homeostasis [8, 9]. Our previous data uncovered some underlying targets of Sr-mediated Ca<sup>2+</sup> metabolism regulation in bovine ruminal epithelial cells [10]. However, it is unknown what effect Sr has on transcription factors (TF) that regulate Ca<sup>2+</sup> metabolism, proliferation, and differentiation.

By binding to enhancer and promoter regions in DNA sequences, TFs play a crucial role in the regulation of gene expression with key functions in numerous cellular processes, such as development and differentiation, stress responses, and response to external signals [11–14]. Research suggested that TFs including the krüppel-like transcriptional factors (KLFs) family, *NRF1*, *SMAD3*, *PPARG*, and *ATF4*, *SIRT4* play roles in the formation and development of bovine adipogenesis, glucose homeostasis, and the regulation of lipid metabolism [15–19]. The TF early growth response 1 (*EGR1*) promotes bovine skeletal muscle-derived satellite cell differentiation, and Sr has the ability to regulate the expression levels of TFs such as *SOX9*, which regulates osteogenic and adipocytic differentiation, articular cartilage degeneration, and subchondral bone remodeling [2, 20–22]. Sr can also inhibit TF such as *PPARG2*, rapidly reducing adipogenesis and thereby suppressing lipid droplet production [23, 24]. Additionally, by inhibiting the *NF-κB* activation, Sr is involved in the anti-inflammatory response and helps

reduce the inflammatory cytokines [25, 26]. Whether Sr is able to affect TFs in ruminal epithelial cells is unknown.

The specific objective of the present study was to use RAN-seq-based transcriptome data to identify the effect of varying doses of Sr on TFs in bovine ruminal epithelial cells. Bioinformatics analysis, including protein-protein interaction networks, and then RT-PCR validation, were used to determine potential biological functions influenced by Sr and the affected TFs.

## Results

### Overview of RNA sequencing results

After removing short raw reads and quality inspection, the RNA sequence produced 53.1, 55.2, 55.6, 54.3, 48.5, and 49.5 million, respectively, clean reads from the six libraries. The GC content percentages were 55.36%, 55.59%, 55.81%, 55.61%, 54.63%, and 55.49%, respectively. The Q20 and Q30 values ranged from 96.90 to 97.22%, 91.56–92.17%, respectively. The reads mapped to the bovine genome all exceeded 96% (Table 1).

### Identification and classification of TFs

As shown in Fig. 1, a total of 1405 TFs were identified and classified into 64 families via an alignment of conserved domains. The *zf-C2H2* family of TFs contains the largest number of genes, followed by TF-Otx and bHLH. Further analysis revealed that the number of DE-TFs was 226, specially 174 DE-TFs showed up-regulated and 52 DE-TFs showed down-regulated (Fig. 2A); the DE-TFs of clustering analysis showed the expression patterns of most TFs (Fig. 2B).

### GSEA analysis of TFs

According to the GSEA-GO results, TFs were mainly enriched in biological processes such as inner ear morphogenesis, inner ear development, membrane part, integral component of membrane, epithelial cell differentiation, and regulation of muscle cell differentiation. Among these biological processes, regulation of muscle cell differentiation was activated ( $P$ -value<0.05), whereas others were inhibited.

According to the GSEA-KEGG results, a total of 28 pathways were enriched ( $P$ -value>0.05) after Sr

**Table 1** Summary of basic statistics for the rumen epithelial cell transcriptome sequencing data

Sample	Raw Datas	Clean Data (%)	Total Mapped (%)	Unique_Mapped(%)	Q20 (%)	Q30 (%)	GC Content (%)
Sr_0–1	53,338,342	53,161,530 (99.67%)	51,471,868 (97.26%)	49,878,179 (94.25%)	97.22%	92.17%	55.36%
Sr_0–2	55,476,744	55,289,308 (99.66%)	53,605,616 (97.38%)	51,902,730 (94.28%)	97.22%	92.15%	55.59%
Sr_0–3	55,825,190	55,631,872 (99.65%)	53,626,105 (96.82%)	51,928,516 (93.76%)	96.91%	91.59%	55.81%
Sr_20–1	54,576,396	54,394,994 (99.67%)	52,501,122 (96.90%)	50,976,998 (94.09%)	96.99%	91.74%	55.61%
Sr_20–2	48,728,294	48,581,650 (99.70%)	46,958,556 (97.08%)	45,603,478 (94.28%)	96.99%	91.63%	54.93%
Sr_20–3	49,708,604	49,544,270 (99.67%)	47,757,597 (96.80%)	46,339,132 (93.93%)	96.90%	91.56%	55.49%

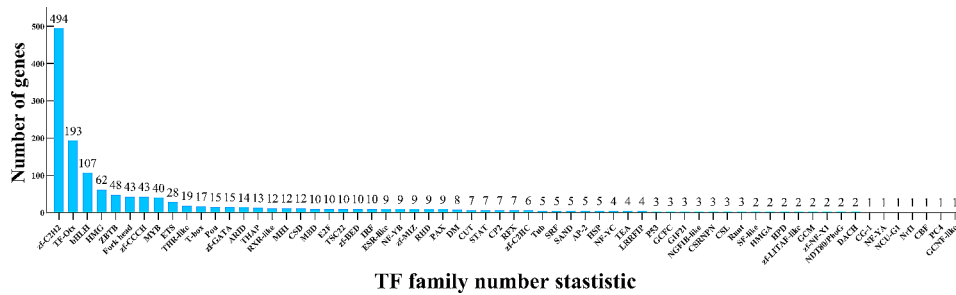


**Fig. 1** Summary of the TF family number statistic. A total of 1405 TFs were identified and classified into 64 families via an alignment of conserved domains

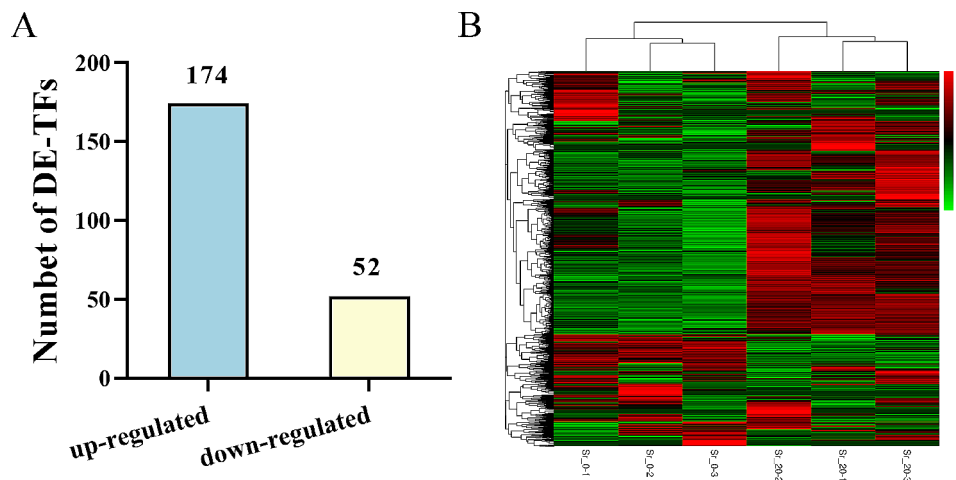


**Fig. 2** Summary of DE-TFs. (A) the number of up-regulated or down-regulated TFs, a total of 226 DE-TFs, specifically 174 DE-TFs showed up-regulated and 52 DE-TFs showed down-regulated; (B) Hierarchical clustering analysis of DE-TFs

treatment, including HTLV-I infection, MAPK signaling pathway, transcriptional misregulation in cancers, hepatocellular carcinoma, and human papillomavirus infection among others (Fig. 3).

**Gene ontology enrichment analysis of DE-TFs**

GO enrichment analysis of DE-TFs revealed 772 GO terms ( $q$ -value<0.05), including 86 terms in molecular function, 42 cellular components, and 644 in biological processes (Fig. 4A). The most significantly enriched terms involved in DNA binding, sequence-specific DNA binding, nucleic acid binding transcription factor activity, transcription factor activity-sequence-specific DNA binding, and sequence-specific double-stranded DNA binding among others (Fig. 4B).

**KEGG pathway analysis of DE-TFs**

DE-TFs were enriched in 135 pathways, a total of 34 of which were significantly enriched according to a  $q$ -value is less than 0.05. The top 20 pathways included the TGF- $\beta$  signaling pathway, transcriptional misregulation in cancer, signaling pathways regulating pluripotency of stem cells, pathways in cancer, human T-cell leukemia virus

1 infection, and Th17 cell differentiation, among others (Fig. 5).

**PPI network construction**

Based on “betweenness”, “closeness”, and “degree”, PPI analysis via STRING and Cytoscape software indicated that the DE-TFs encompassed a total of 49 core targets (Fig. 6). A total of 12 hub DE-TFs were detected, among which the expression levels of *SMAD4*, *SMAD2*, *SPI*, *LEF1*, *ETS1*, *NR3C1*, *SMAD3*, *FOXO1*, *MEF2A*, and *NCOA2* were up-regulated, while the expression levels of *PPARG* and *GATA2* were down-regulated (Fig. 7).

**Verification of DE-TFs by RT-PCR**

The results of RT-PCR for 12 selected TFs are in Fig. 8. The *SMAD2* and *MEF2A* expression levels were up-regulated after treatment with Sr for 24 h. The expression of *LEF1* and *NCOA2* were up-regulated in response to 10 and 20 mmol/L Sr group. The *ETS1* was up-regulated in the 20 mmol/L Sr group. The expression levels of *PPARG*, *NR3C1*, *GATA2*, and *SMAD3* were up-regulated in the 1 mmol/L group and down-regulated in the 20 mmol/L group. The *FOXO1* expression level was down-regulated in the 10 and 20 mmol/L groups, the *SMAD4* expression

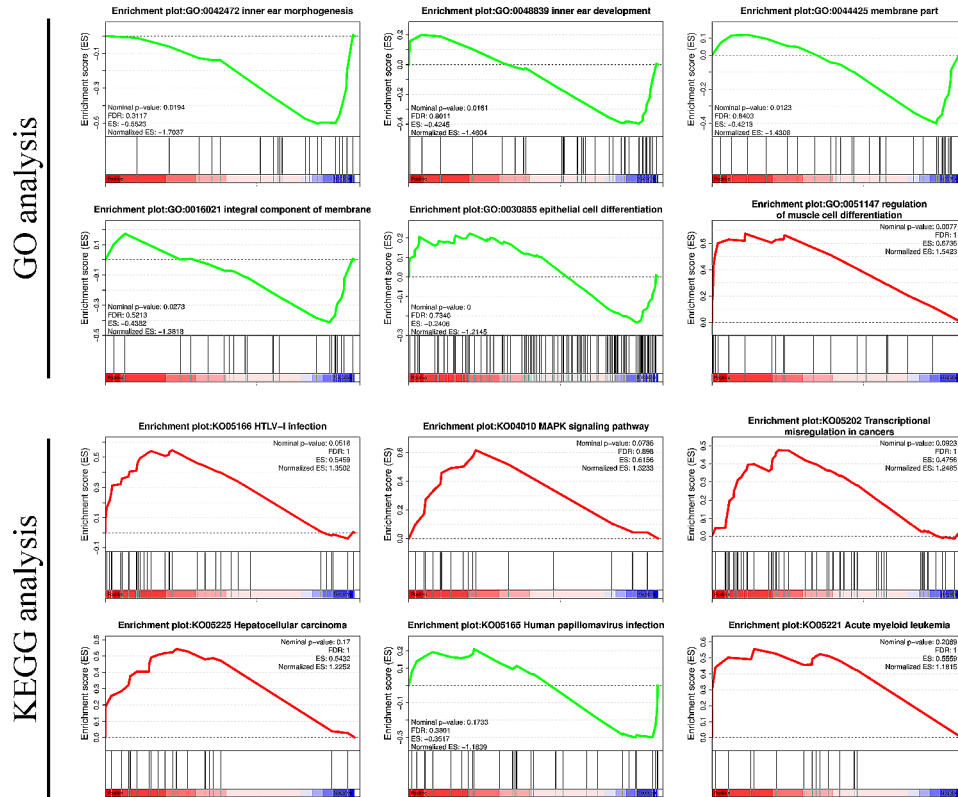


**Fig. 3** GSEA analysis results. The GSEA-GO results showed that among these biological processes, regulation of muscle cell differentiation was activated ( $P$ -value < 0.05), whereas others were inhibited. the GSEA-KEGG results showed that a total of 28 pathways were enriched ( $P$ -value > 0.05)

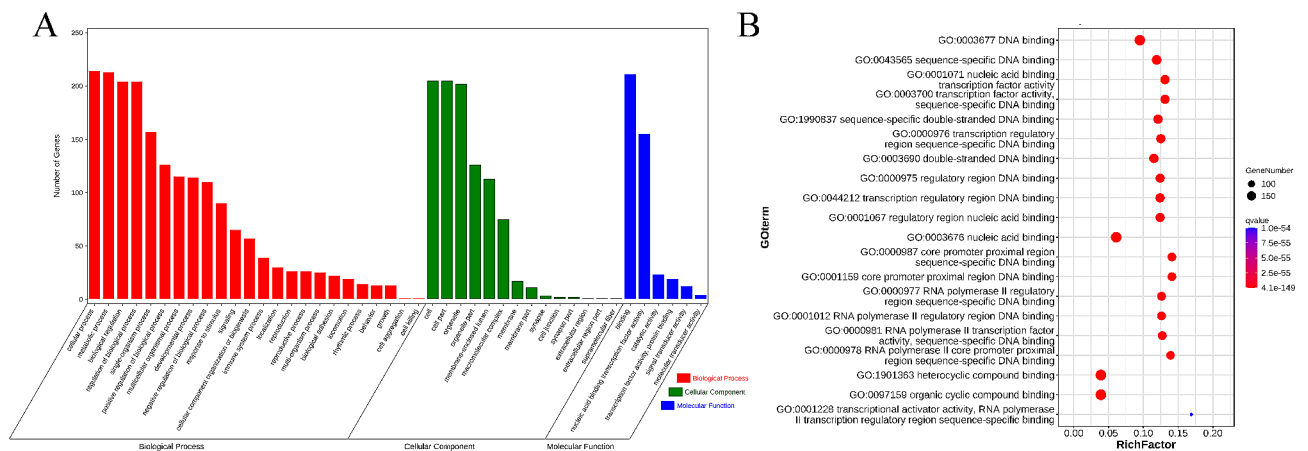


**Fig. 4** GO enrichment of DE-TFs. (A) The barplot of GO enrichment, mainly enriched in biological process; (B) The bubble chart of GO enrichment, the most significantly enriched terms involved in DNA binding, sequence-specific DNA binding, and nucleic acid binding transcription factor activity among others

level was down-regulated in the 20 mmol/L group, while the expression level of *SP1* was not affected by Sr treatment.

RT-PCR and RNA-seq analysis of *GATA2*, *ETS1*, *MEF2A*, *SMAD2*, *PPARG*, *LEF1*, and *NCOA2* in 20 mmol/L groups show a consistent expression changes, while the expression changes of *SMAD4*, *SMAD3*, and

*FOXO1* detected by RT-PCR and RNA-seq display an opposite trends.

### Discussion

Transcription factors recognize specific DNA sequences to control chromatin and transcription, thus, play an important role in a wide variety of processes, including the regulation of gene expression, cellular function, and

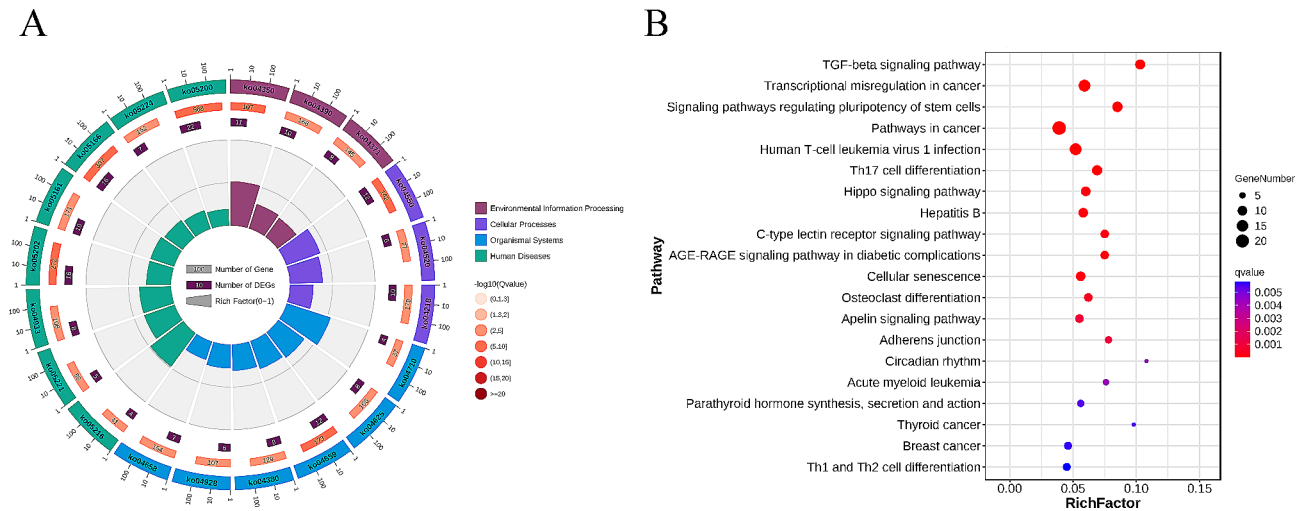


**Fig. 5** KEGG pathway enrichment of DE-TFs. **(A)** The circos plot of KEGG pathway enrichment, mainly enriched in human diseases, and organismal systems; **(B)** The bubble chart of KEGG pathway enrichment, 34 of which were significantly enriched ( $P$ -value < 0.05) in the TGF- $\beta$  signaling pathway, transcriptional misregulation in cancer among others

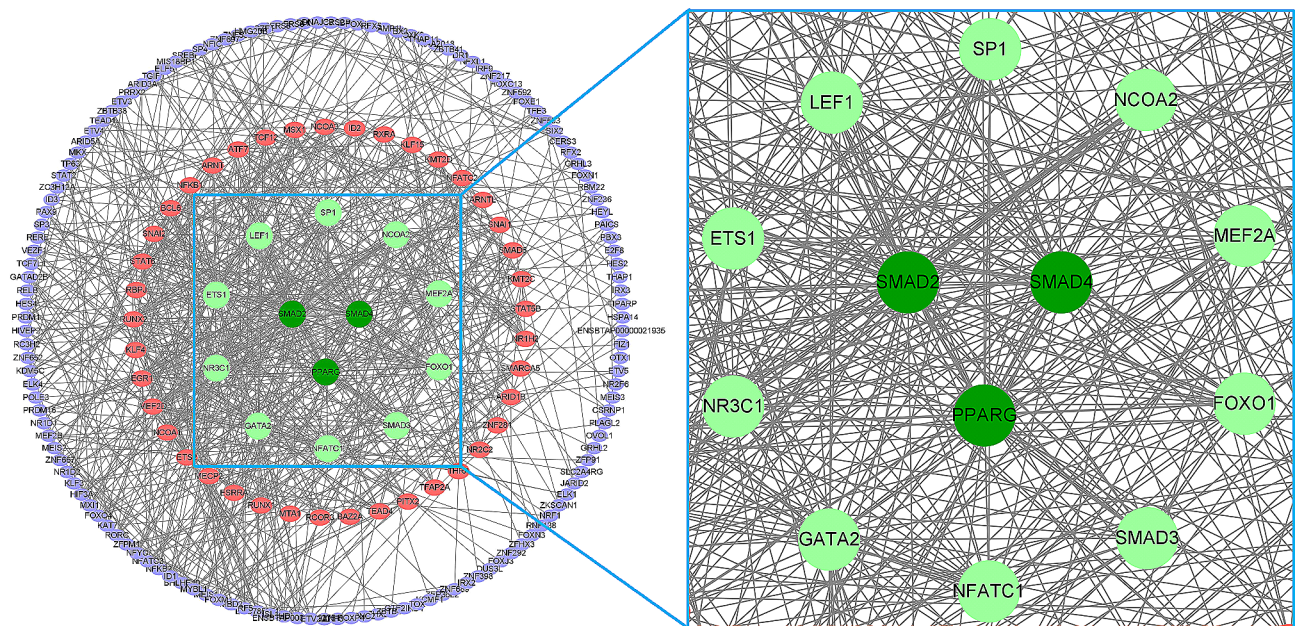


**Fig. 6** Screen of hub DE-TFs. PPI analysis showed that the DE-TFs encompassed a total of 49 core targets, with a total of 12 hub DE-TFs were detected, including *PPARG*, *SMAD4*, *SMAD2*, *SMAD3*, *FOXO1*, *MEF2A*, *NCOA2*, *SP1*, *LEF1*, *ETS1*, *NR3C1*, and *GATA2*

environmental responses [27, 28]. The AnimalTFDB v4.0 website contains information for 1445 TFs and 939 TF Cofactors for *Bos taurus*. From the sequencing results, we identified 1405 TFs classified into 64 families, among which *Zf-C2H2*, *TF-Otx*, and *bHLH* were dominant after Sr treatment. GO enrichment analysis of 226 DE-TFs revealed that “binding” was the highest GO category with DNA binding having 192 transcription factors, sequence-specific DNA binding having 165 transcription factors, and nucleic acid binding having 155 transcription factors. Such associations likely reflect the fact that

all transcriptional events in living organisms require the binding of polyprotein complexes to DNA [29].

The KEGG enrichment analysis revealed that DE-TFs were enriched in pathways such as TGF- $\beta$  signaling pathway, transcriptional misregulation in cancer, signaling pathways regulating pluripotency of stem cells, pathways in cancer, human T-cell leukemia virus 1 infection, and Th17 cell differentiation among others. TFs are involved in cell progression, such as cell differentiation, cell proliferation, response to external signals, among others, through regulating the expression of regulatory genes

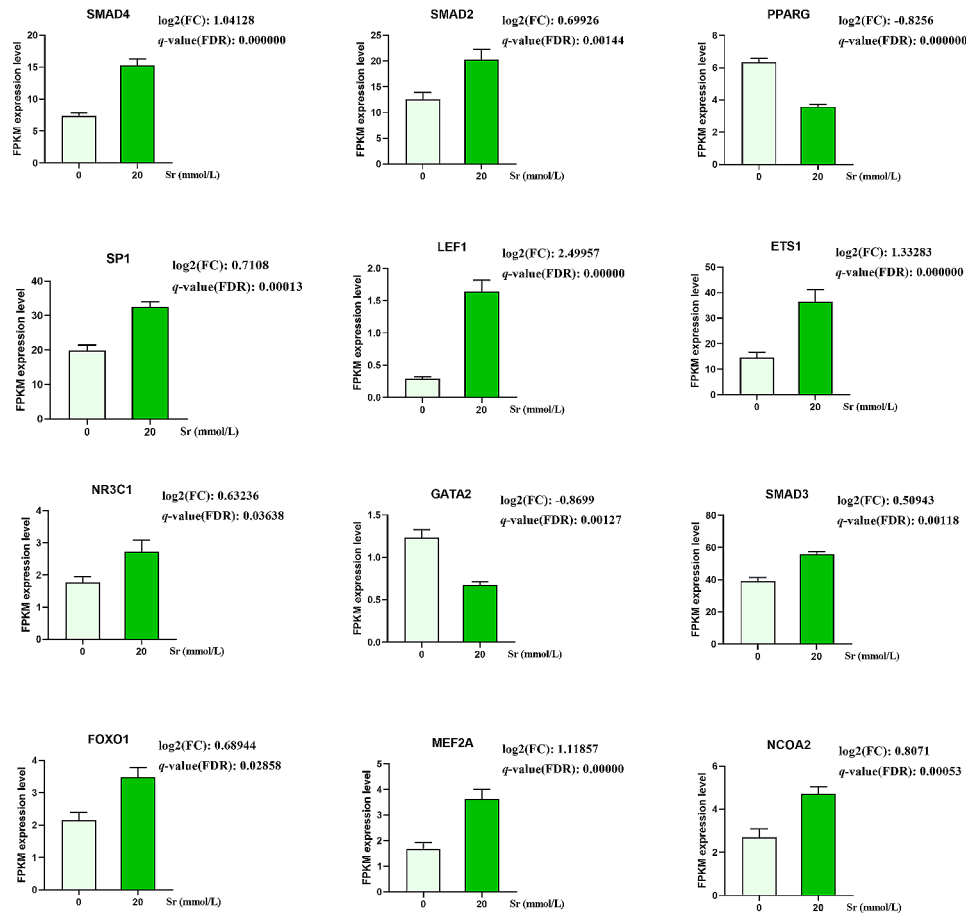


**Fig. 7** The hub DE-TFs expression levels in RNA-seq. The expression levels of *SMAD4*, *SMAD2*, *SP1*, *LEF1*, *ETS1*, *NR3C1*, *SMAD3*, *FOXO1*, *MEF2A* and *NCOA2* were up-regulated ( $q$ -value < 0.01 and  $q$ -value < 0.05), while the expression levels of *PPARG* and *GATA2* were down-regulated ( $q$ -value < 0.01)

and all other genes [11–13]. Thus, it was important to explore hub TFs in response to treatment with Sr. The PPI analysis of DE-TFs after treatment with Sr revealed 12 hub-TFs: *SMAD4*, *SMAD2*, *SMAD3*, *SP1*, *GATA2*, *NR3C1*, *PPARG*, *FOXO1*, *MEF2A*, *NCOA2*, *LEF1*, and *ETS1*.

The TGF- $\beta$  superfamily signaling regulates several cellular processes including cell differentiation, proliferation, apoptosis, inflammation, and fibrosis [30, 31]. SMAD proteins are the central players in the canonical TGF- $\beta$  signaling pathway in which signaling triggers the phosphorylation of the receptor-activated SMADs (R-SMADs), *SMAD2* and *SMAD3* [32]. The activated R-SMADs bind the common mediator SMAD (co-SMAD), *SMAD4*, and the resulting complexes relocate into the nucleus [33–35]. For instance, a previous study reported that Sr increased the *SMAD2/3* and TGF- $\beta$  protein expression levels and regulated the TGF- $\beta$ /SMAD signaling pathway to promote osteogenic differentiation [36]. Similarly, our previous study observed that Sr regulated primary chondrocyte proliferation

and differentiation by directing TGF $\beta$ 1 signaling toward *SMAD3* phosphorylation [7].

Through binding to *SMAD4*, *GATA2* acts as a negative regulator of the TGF- $\beta$  signaling pathway, and its overexpression decreases the DNA binding activity of *SMAD4* [37]. *ETS1* plays a role in osteoblast differentiation and bone development and is a downstream signaling effector for several TGF $\beta$ 1 responsive genes [38, 39]. Overexpression of *ETS1* prevented the TGF- $\beta$ -induced reduction in DNA-binding activity [40]. Myocyte enhancer factor 2 A (*MEF2A*) inhibition abated activation of the TGF- $\beta$ /SMAD signaling pathways [41]. The overexpression of specificity protein 1 (*SP1*) increased TGF- $\beta$ 1 expression levels and activated the TGF- $\beta$ 1/SMAD2 signaling pathway, while the downregulation of *SP1* inhibited osteoblast differentiation [42, 43].

In the present study, the expression levels of *SMAD2*, *ETS1*, and *MEF2A* were significantly increased ( $P < 0.01$  and  $P < 0.05$ ) and the *GATA2* was significantly decreased ( $P < 0.05$ ), which was consistent in RT-PCR and RNA-seq. However, the decreased expression levels *SMAD4* and *SMAD3* ( $P < 0.05$ ) and the unchanged *SP1* as shown

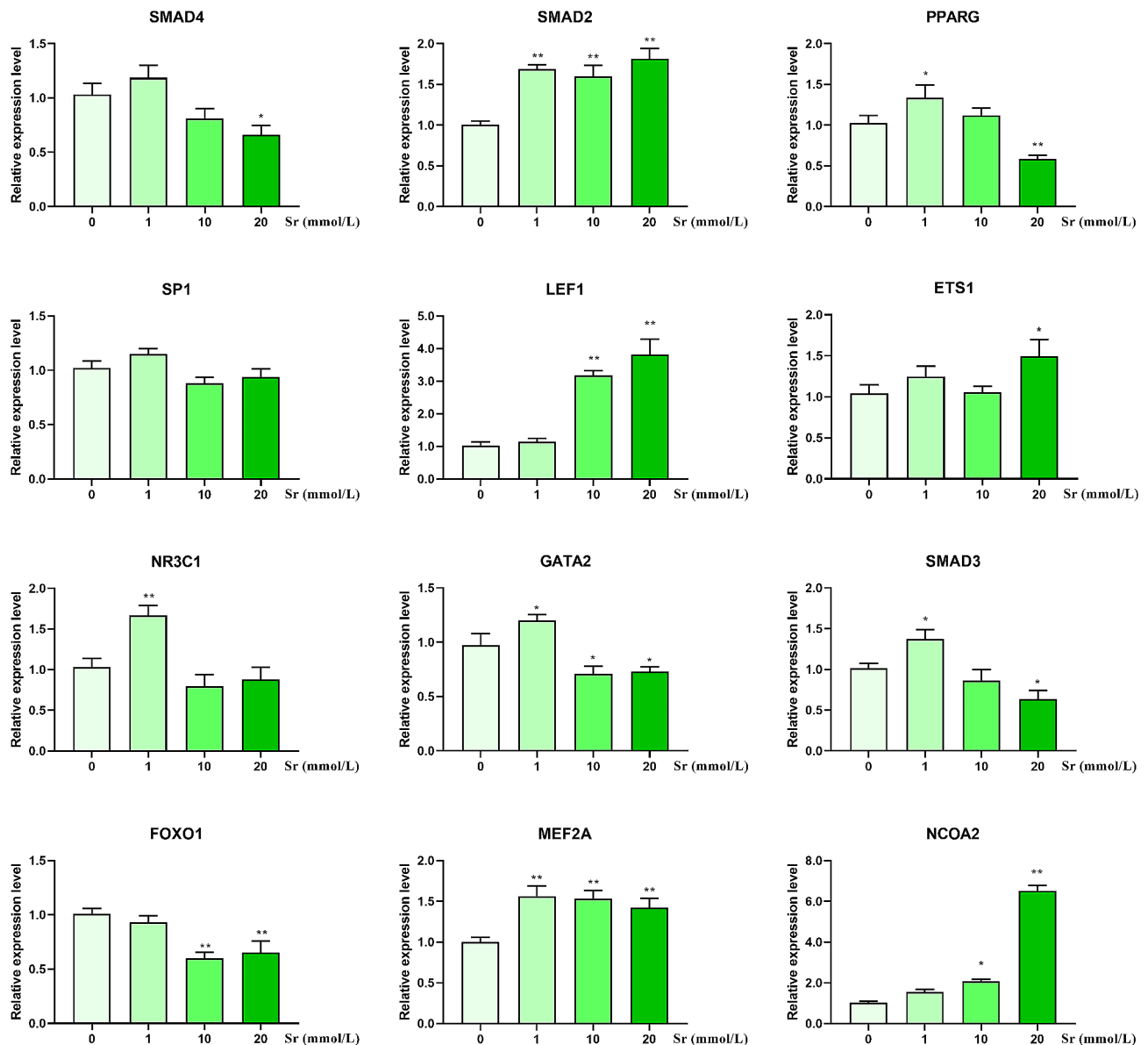


**Fig. 8** mRNA expression analysis of 12 DE-TFs genes at different doses of Sr. Data are presented as mean  $\pm$  SEM, \* $P < 0.05$ , \*\* $P < 0.01$  as compared with the 0 mmol/L Sr group

in RT-PCR were opposite to RNA-seq likely due to the interference of duplication in the sequencing results. Based on the GSEA analysis of TFs, KEGG enrichment analysis of DE-TFs and RT-PCR analysis, the altered expression levels of *SMAD2*, *ETS1*, *GATA2*, and *MEF2A* indicated that Sr may activate the TGF- $\beta$  signaling pathway to regulate the differentiation of ruminal epithelial cells. The precise molecular mechanisms require further investigation.

The ruminal epithelium is the main site for ketogenesis from acetate and butyrate during the fed state, while in non-ruminants and ruminants ketogenesis occurs mainly in the liver during the post-absorptive or starvation states [44]. Both *PPARG* and *FOXO1* are regulatory

proteins that play a crucial role in lipid metabolism [45–47]. *FOXO1* binds directly to the promoter of *PPARG* resulting in the suppression of its transcription, thereby decreasing adipogenesis [45, 48]. The overexpression of *FOXO1* in liver contributes to an increase in the synthesis of triglyceride (TGs) and a decrease in the oxidation of fatty acids, exacerbating hepatic steatosis [49]. *PPARG* serves as the main regulator of triacylglycerol synthesis and secretion, and its overexpression indeed induces lipid accumulation [50]. *NCOA2* (also referred to as *TIF2*), an activator of *PPARG*, is a master TF of adipogenesis and its knockdown can decrease *PPARG* activity thereby reducing fat accumulation in white adipose tissue [51–53]. Glucocorticoid receptor (*NR3C1*),

a glucocorticoid receptor, is a modulator of hormonal regulation of immunity and lipid metabolism, and glucocorticoids up-regulate *FOXO1* expression by binding to *NR3C1* [54, 55]. Lymphocyte enhancer factor-1 (*LEF1*) is a member of the LEF1/T-cell factor (TCF) family, and it could interact with *β-catenin* to regulate adipogenesis and negatively regulate lipid deposition [56, 57].

In this study, the decreased expression of *PPARG* ( $P < 0.01$ ) and the increased expression of *NCOA2* and *LEF1* expression levels ( $P < 0.01$ ), were consistent in RT-PCR and RNA-seq. However, the *FOXO1* expression levels were decreased ( $P < 0.01$ ) and the *NR3C1* expression levels were not significantly changed in the results of RT-PCR were opposite to RNA-seq for reasons that cannot be explained with the available data. The altered expression of *PPARG* and *LEF1* indicated that Sr plays an important role in lipid metabolism in ruminal epithelial cells.

## Conclusions

A large number of TFs were identified by RNA-seq in response to incubation with Sr, suggesting they may be involved in different regulatory pathways in ruminal epithelial cells. Seven potential targets for Sr-mediated cell proliferation and differentiation, and lipid metabolism regulation were identified: *SMAD2*, *PPARG*, *LEF1*, *ETS1*, *GATA2*, *MEF2A*, and *NCOA2*. Understanding the underlying molecular mechanisms of these TFs requires further studies. Overall, the results enhanced the knowledge regarding the impacts of Sr on transcriptional regulation in ruminal epithelial cells. Whether Sr could be used in practice to alter molecular mechanisms in vivo will have to be addressed in future research.

## Materials and methods

### Primary bovine rumen epithelial cells isolation, culture and treatment

The primary bovine ruminal epithelial cells were isolated as previously described [10, 58]. In brief, the newborn Holstein male calves ( $n = 3$ ,  $38.0 \pm 2.8$  kg body weight) were euthanized with veterinarian pentobarbital sodium at 100 mg/kg intravenous. The rumen tissue was collected and washed several times until no visible rumen contents remained. Then, the ruminal epithelium was bluntly dissected and washed with PBS buffer containing penicillin, streptomycin, and amphotericin B, gentamicin. The ruminal epithelium was aseptically cut into small pieces ( $3\text{--}4\text{ cm}^2$ ) and trypsinized via serial incubations with trypsin-EDTA solution. The subsequent 4 fractions of supernatant were each strained through 50-mesh and washed with PBS buffer. Then, the ruminal epithelium cell pellet was resuspended with DMEM-low-glucose medium and strained through 200-mesh. Lastly, the cell density was adjusted to  $1 \times 10^6$  cells/mL, and seeded into

six-well cell culture plates (2 mL per well) followed by incubation at 37 °C in 5% CO<sub>2</sub> in a humidified incubator. The medium was changed every 2 days.

According to the IC50, cell cycle, and Ca<sup>2+</sup> levels in our previous study, primary bovine ruminal epithelium cells were cultured up to 90% confluency, the original culture medium was discarded, and the cells were washed with PBS buffer. The fresh medium containing different doses of Sr (0, 1, 10, and 20 mmol/L) was added to the corresponding groups, and the cells were cultured in a 5% CO<sub>2</sub> atmosphere at 37 °C for 24 h (three replicates for each group). Then the cells were washed twice with PBS buffer, collected by scraping with a cell scraper, and stored at -80 °C to be used for subsequent experiments.

### RNA isolations, libraries construction and sequencing

Total RNA from the experimental cells was extracted using TRIzol™ Reagent (Invitrogen, Carlsbad, CA, USA) according to the recommendations. After evaluation of the RNA quality assessed by Agilent 2100 Bioanalyzer (Agilent Technologies, Palo Alto, CA, USA) and checked using RNase free agarose gel electrophoresis, mRNA was enriched by Oligo(dT) beads. Then the enriched mRNA was fragmented into short fragments and reversed transcribed into cDNA by using NEBNext Ultra RNA Library Prep Kit for Illumina (NEB#7530, New England Biolabs, Ipswich, MA, USA). After synthesis of the second strand cDNA, fragments were end repaired and ligated to Illumina sequencing adapters. The ligation reaction was purified with the AMPure XP Beads (1.0X). Ligation products cDNA were size-selected by agarose gel electrophoresis and amplified by PCR, then the PCR products were purified with AMPure XP beads (1.0X), and the cDNA library was obtained. The resulting cDNA library was assessed the quality testing by agarose gel electrophoresis, NanoPhotometer spectrophotometer (Thermo Fisher Scientific, Massachusetts, USA), Qubit2.0 Fluorometer (Thermo Fisher Scientific, Massachusetts, USA), and Agilent 2100 bioanalyzer (Agilent Technologies, Palo Alto, CA, USA), and then sequenced using Illumina Novaseq6000 by Gene Denovo Biotechnology Co.(Guangzhou, China). The RNA-seq datasets were deposited in the NCBI Sequence Read Archive (SRA) with accession number SUB12106664.

RNA differential expression analysis was performed via DESeq2 software between two different groups. The genes with the parameter of false discovery rate (FDR) below 0.05 were considered differentially expressed gene (DEG).

### Identification of TFs

Unigenes that were annotated as transcription factor genes, for instance, bZIP, bHLH, and MYB, were then selected for further analysis. The differentially expressed



transcription factor genes and identified temporal expression profiles were evaluated by the Short Time-series Expression Miner V1.3.13 (STEM) program.

### Functional GO and KEGG analysis

The functional analysis (GO and KEGG pathway) of DE-TFs was performed using the OmicShare tools at [www.omicshare.com/tools](http://www.omicshare.com/tools).  $q$ -value is the  $P$ -value after multiple verification, and the GO function or KEGG pathway is considered to be significantly enriched if the  $q$ -value is less than 0.05.

A PPI was generated using STRING (<https://cn.string-db.org/>) and Cytoscape software (version 3.8.2) diagram to present the core and the biological interaction of hub genes.

### Gene set enrichment analysis (GSEA)

GSEA analysis was performed by using software GSEA and MSigDB to identify whether a set of genes in specific GO terms/KEGG pathways shows significant differences in control and Sr 20 mmol/L groups ([www.omicshare.com/tools](http://www.omicshare.com/tools)).

### Quantitative real-time polymerase chain reaction

After the total RNA was extracted, the cDNA was produced by reverse-transcribing the isolated total RNA using the FastKing RT Kit With gDNase (TIANGEN, Beijing). RT-PCR was performed in triplicate by using SYBR Green RT-PCR Master Mix (Vazyme, Nanjing). Primers were designed from span introns using NCBI primer design tool. The detailed primer information were shown in supplementary materials Table S1. *GAPDH* and  *$\beta$ -actin* were used as dual endogenous control. Relative quantification was done using the  $2^{-\Delta\Delta CT}$  method.

### Statistical analysis

RNA-seq analysis: the raw reads were filtered by fastp (version 0.18.0) and base quality analysis to clean data, the clean data were blasted to the ribosomal RNA for unmapped reads; then the unmapped reads were aligned with the reference genome mapped to the *Bos taurus* reference genome (Ensembl\_release104) using HISAT2. 2.4 software (<http://www.ccb.jhu.edu/software/hisat/> accessed on 15 August 2021). The unmapped reads of each sample were assembled using StringTie v1.3.1 (<https://ccb.jhu.edu/software/stringtie/> accessed on 15 August 2021) in a reference-based approach. A fragment per kilobase of transcript per million mapped reads (FPKM) value was calculated to quantify its expression abundance and variations, using RSEM software. RNA differential expression analysis was performed with DESeq2 (version 1.40.1) software between the 0 mmol/L (Sr-0) and 20 mmol/L (Sr-20) Sr treatment groups.

All results are presented as mean  $\pm$  standard deviation (SEM). GraphPad Prism 5.01 software and Statistical Package for the Social Sciences (SPSS 17.0) packages were used for statistical analyses. The  $P$  values were determined using one-way ANOVA among the various groups, and statistically significant was determined at  $P < 0.05$ .

### Abbreviations

DEG	Differentially expressed gene
DE-TFs	Differentially expressed TFs
RT-PCR	Real-time polymerase chain reaction
SMAD4	SMAD family member 4
SMAD2	SMAD family member 2
SMAD3	SMAD family member 3
SP1	Specificity protein 1
GATA2	GATA binding protein 2
NR3C1	Glucocorticoid receptor
PPARG	Peroxisome proliferator-activated receptor-gamma
FOXO1	Forkhead box-O1
MEF2A	Myocyte enhancer factor 2 A
NCOA2	Nuclear receptor coactivator 2
LEF1	Lymphocyte enhancer factor-1
ETS1	ETS proto-onco 1
TGs	Triglyceride

### Supplementary Information

The online version contains supplementary material available at <https://doi.org/10.1186/s12917-024-03929-9>.

**Supplementary Material 1: Table S1** Sequences used for RT-PCR

### Acknowledgements

The authors would like to thank the support of the China National Natural Science Foundation and Department of Science and Technology of Shaanxi Province, and thank the editors and reviewers for their critical reading and constructive suggestions.

### Author contributions

PT carried out the experiments, analysed the data and drafted the manuscript. LM and FZ prepared samples and helped in laboratory analysis. LM and YK helped with the preparation/submission of the manuscript materials. YW, CZ and JJ L contributed to the experimental design, supervised the study, and revised the manuscript. BZ and JW was a contributed to the experimental design, supervised the study, and revised the manuscript. All authors read and final version of the manuscript.

### Funding

This work was supported by the National Natural Science Foundation of China (grant numbers 32273085, 32102742), the National Key R&D Program of China (grant numbers 2023YFD1801100), and the Key Research and Development Program of Shaanxi (grant numbers 2021NY-022).

### Data availability

The raw Illumina sequencing data were archived in the NCBI Sequence Read Archive (NCBI SRA) under accession number SUB12106664.

### Declarations

#### Ethics approval and consent to participate

This study was conducted in Western China (106°55'57"E, 34°48'41"N) at the experimental farm of Northwest A&F University (Shaanxi Province, China). The animal experimental protocol adopted in this study was approved by the Animal Ethical and Welfare Committee Ethics, Northwest A&F University, China, and was conducted in accordance with the university's guidelines for animal research (Approval No. 2021049).

**Consent for publication**

Not applicable.

**Competing interests**

The authors declare no competing interests.

Received: 21 September 2023 / Accepted: 9 February 2024

Published online: 08 March 2024

**References**

- Lin SJ, Huang CC. Strontium peroxide-loaded composite scaffolds capable of Generating Oxygen and modulating behaviors of osteoblasts and osteoclasts. *Int J Mol Sci*. 2022;23(11):6322.
- Li YQ, Yue JH, Liu Y, Wu J, Guan M, Chen D, et al. Strontium regulates stem cell fate during osteogenic differentiation through asymmetric cell division. *Acta Biomater*. 2021;119:432–43.
- Rossi AL, Moldovan S, Querido W, Rossi A, Werckmann J, Ersen O, et al. Effect of strontium ranelate on bone mineral: analysis of nanoscale compositional changes. *Micron*. 2014;56:29–36.
- Alexandersen P, Karsdal MA, Byrjalsen I, Christiansen C. Strontium ranelate effect in postmenopausal women with different clinical levels of osteoarthritis. *Climacteric*. 2011;14(2):236–43.
- Cheng Y, Huang L, Wang Y, Huo Q, Shao Y, Bao H, et al. Strontium promotes osteogenic differentiation by activating autophagy via the the AMPK/mTOR signaling pathway in MC3T3–E1 cells. *Int J Mol Med*. 2019;44(2):652–60.
- Tsai SW, Hsu YW, Pan WL, Hsu FY. The Effect of Strontium-substituted Hydroxyapatite Nanofibrous Matrix on osteoblast proliferation and differentiation. *Membr (Basel)*. 2021;11(8):624.
- Liu S, Shen B, Looor JJ, Jiang Q, Yuan Y, Kong Y, et al. Strontium regulates the proliferation and differentiation of isolated primary bovine chondrocytes via the TGFbeta/SMAD pathway. *Front Pharmacol*. 2022;13:925302.
- Hyde ML, Wilkens MR, Fraser DR. In vivo measurement of strontium absorption from the rumen of dairy cows as an index of calcium absorption capacity. *J Dairy Sci*. 2019;102(6):5699–705.
- Hyde ML, Fraser DR. In vivo measurement of the absorption of strontium in the rumen and small intestine of sheep as an index of calcium absorption capacity. *Brit J Nutr*. 2014;112(5):718–24.
- Tan P, Zhao C, Dong Y, Zhang Z, Mei L, Kong Y, et al. A Network Pharmacology and Multi-omics Combination Approach to reveal the Effect of Strontium on Ca2+ metabolism in bovine rumen epithelial cells. *Int J Mol Sci*. 2023;24(11):9383.
- Zhang J, Guo F, Zhou R, Xiang C, Zhang Y, Gao J, et al. Proteomics and transcriptome reveal the key transcription factors mediating the protection of Panax notoginseng saponins (PNS) against cerebral ischemia/reperfusion injury. *Phytomedicine*. 2021;92:153613.
- Thakur V, Bains S, Pathania S, Sharma S, Kaur R, Singh K. Comparative transcriptomics reveals candidate transcription factors involved in costunolide biosynthesis in medicinal plant-Saussurea lappa. *Int J Biol Macromol*. 2020;150:52–67.
- Weidemuller P, Kholmatov M, Petsalaki E, Zaugg JB. Transcription factors: bridge between cell signaling and gene regulation. *Proteomics*. 2021;21(23–24):e2000034.
- Huang Y, Kong Y, Li B, Zhao C, Looor JJ, Tan P, et al. Effects of perinatal stress on the metabolites and lipids in plasma of dairy goats. *Stress Biol*. 2023;3(1):11.
- Hong J, Li S, Wang X, Mei C, Zan L. Study of expression analysis of SIRT4 and the coordinate regulation of bovine adipocyte differentiation by SIRT4 and its transcription factors. *Biosci Rep*. 2018;38(6):BSR20181705.
- Khan R, Raza SHA, Schreurs N, Wang XY, Wang HB, Ullah I, et al. Bioinformatics analysis and transcriptional regulation of TORC1 gene through transcription factors NRF1 and Smad3 in bovine preadipocytes. *Genomics*. 2020;112(2):1575–87.
- Raza SHA, Pant SD, Wani AK, Mohamed HH, Khalifa NE, Almohameed HM, et al. Kruppel-like factors family regulation of adipogenic markers genes in bovine cattle adipogenesis. *Mol Cell Probe*. 2022;65:101850.
- Wei X, Han S, Wang S, Zheng Q, Li X, Du J, et al. ANGPTL8 regulates adipocytes differentiation and adipogenesis in bovine. *Gene*. 2019;707:93–9.
- Huang Y, Zhao C, Liu Y, Kong Y, Tan P, Liu S, et al. NEFA promotes autophagosome formation through modulating PERK signaling pathway in bovine hepatocytes. *Anim (Basel)*. 2021;11(12):3400.
- Zhang W, Tong H, Zhang Z, Shao S, Liu D, Li S, et al. Transcription factor EGR1 promotes differentiation of bovine skeletal muscle satellite cells by regulating MyoG gene expression. *J Cell Physiol*. 2018;233(1):350–62.
- Yu DG, Ding HF, Mao YQ, Liu M, Yu B, Zhao X, et al. Strontium ranelate reduces cartilage degeneration and subchondral bone remodeling in rat osteoarthritis model. *Acta Pharmacol Sin*. 2013;34(3):393–402.
- Li Y, Li J, Zhu S, Luo E, Feng G, Chen Q, et al. Effects of strontium on proliferation and differentiation of rat bone marrow mesenchymal stem cells. *Biochem Biophys Res Commun*. 2012;418(4):725–30.
- Fournier C, Perrier A, Thomas M, Laroche N, Dumas V, Rattner A, et al. Reduction by strontium of the bone marrow adiposity in mice and repression of the adipogenic commitment of multipotent C3H10T1/2 cells. *Bone*. 2012;50(2):499–509.
- Zhou C, Chen YQ, Zhu YH, Lin GF, Zhang LF, Liu XC, et al. Antiadipogenesis and Osseointegration of Strontium-Doped Implant surfaces. *J Dent Res*. 2019;98(7):795–802.
- Zhu SJ, Hu XY, Tao YX, Ping ZC, Wang LL, Shi JW, et al. Strontium inhibits titanium particle-induced osteoclast activation and chronic inflammation via suppression of NF-kappa B pathway. *Sci Rep-Uk*. 2016;6:36251.
- Tan P, Yang J, Yi F, Mei L, Wang Y, Zhao C, et al. Strontium attenuates LPS-induced inflammation via TLR4/MyD88/NF-kB pathway in bovine ruminal epithelial cells. *Biol Trace Elem Res*. 2023. <https://doi.org/10.1007/s12011-023-03992-7>.
- Wang Y, Chen R, Wang Q, Yue Y, Gao Q, Wang C, et al. Transcriptomic analysis of large yellow croaker (*Larimichthys crocea*) during early development under hypoxia and acidification stress. *Vet Sci*. 2022;9(11):632.
- Xiu YJ, Li YR, Liu XF, Li C. Full-length transcriptome sequencing from multiple immune-related tissues of Paralichthys olivaceus. *Fish Shellfish Immun*. 2020;106:930–7.
- Beckett D. Regulated assembly of transcription factors and control of transcription initiation. *J Mol Biol*. 2001;314(3):335–52.
- Li SN, Wu JF. TGF-beta/SMAD signaling regulation of mesenchymal stem cells in adipocyte commitment. *Stem Cell Res Ther*. 2020;11(1):41.
- Aashaq S, Batool A, Mir SA, Beigh MA, Andrabi KI, Shah ZA. TGF-beta signaling: a recap of SMAD-independent and SMAD-dependent pathways. *J Cell Physiol*. 2022;237(1):59–85.
- Chai N, Li WX, Wang J, Wang ZX, Yang SM, Wu JW. Structural basis for the Smad5 MH1 domain to recognize different DNA sequences. *Nucleic Acids Res*. 2015;43(18):9051–64.
- Jones JB, Kern SE. Functional mapping of the MH1 DNA-binding domain of DPC4/SMAD4. *Nucleic Acids Res*. 2000;28(12):2363–8.
- Shu X, Shu SY, Cheng HQ. Genome-wide mRNA-Seq profiling reveals that LEF1 and SMAD3 regulate epithelial-mesenchymal transition through the Hippo Signaling Pathway during Palatal Fusion. *Genet Test Mol Bioma*. 2019;23(3):197–203.
- Fleming NI, Jorissen RN, Mouradov D, Christie M, Sakthianandeswaren A, Palmieri M, et al. SMAD2, SMAD3 and SMAD4 mutations in colorectal cancer. *Cancer Res*. 2013;73(2):725–35.
- Liu Z, Yu Z, Chang H, Wang Y, Xiang H, Zhang X, et al. Strontium-containing alpha-calcium sulfate hemihydrate promotes bone repair via the TGF-beta/Smad signaling pathway. *Mol Med Rep*. 2019;20(4):3555–64.
- Dong XM, Yin RH, Yang Y, Feng ZW, Ning HM, Dong L, et al. GATA-2 inhibits transforming growth factor-beta signaling pathway through interaction with Smad4. *Cell Signal*. 2014;26(5):1089–97.
- Qi MC, Hu J, Zou SJ, Chen HQ, Zhou HX, Han LC. Mechanical strain induces osteogenic differentiation: Cbfa1 and Ets-1 expression in stretched rat mesenchymal stem cells. *Int J Oral Maxillofac Surg*. 2008;37(5):453–8.
- Raouf A, Seth A. Ets transcription factors and targets in osteogenesis. *Oncogene*. 2000;19(55):6455–63.
- Geisinger MT, Astaiza R, Butler T, Popoff SN, Planey SL, Arnott JA. Ets-1 is essential for connective tissue growth factor (CTGF/CEN2) induction by TGF-beta 1 in Osteoblasts. *PLoS ONE*. 2012;7(4):e35258.
- Chen X, Liu G, Zhang W, Zhang J, Yan Y, Dong W, et al. Inhibition of MEF2A prevents hyperglycemia-induced extracellular matrix accumulation by blocking Akt and TGF-beta1/Smad activation in cardiac fibroblasts. *Int J Biochem Cell Biol*. 2015;69:52–61.
- Ding A, Bian YY, Zhang ZH. SP1/TGF-beta 1/SMAD2 pathway is involved in angiogenesis during osteogenesis. *Mol Med Rep*. 2020;21(3):1581–9.
- Sohrabi SS, Sohrabi SM, Rashidipour M, Mohammadi M, Khalili Fard J, Mirzaei Najafgholi H. Identification of common key regulators in rat hepatocyte cell lines under exposure of different pesticides. *Gene*. 2020;739:144508.

44. Ji X, Tong H, Settlage R, Yao W, Jiang H. Establishment of a bovine rumen epithelial cell line. *J Anim Sci*. 2021;99(10):kab273.
45. Li Y, Ma Z, Jiang S, Hu W, Li T, Di S, et al. A global perspective on FOXO1 in lipid metabolism and lipid-related diseases. *Prog Lipid Res*. 2017;66:42–9.
46. Sikder K, Shukla SK, Patel N, Singh H, Rafiq K. High Fat Diet upregulates fatty acid oxidation and ketogenesis via intervention of PPAR-gamma. *Cell Physiol Biochem*. 2018;48(3):1317–31.
47. Galbraith L, Leung HY, Ahmad I. Lipid pathway deregulation in advanced prostate cancer. *Pharmacol Res*. 2018;131:177–84.
48. Kohan K, Carvajal R, Gabler F, Vantman D, Romero C, Vega M. Role of the transcriptional factors FOXO1 and PPARG on gene expression of SLC2A4 in endometrial tissue from women with polycystic ovary syndrome. *Reproduction*. 2010;140(1):123–31.
49. Matsumoto M, Han S, Kitamura T, Accili D. Dual role of transcription factor FoxO1 in controlling hepatic insulin sensitivity and lipid metabolism. *J Clin Invest*. 2006;116(9):2464–72.
50. Kang Y, Hengbo S, Jun L, Jun L, Wangsheng Z, Huibin T, et al. PPARG modulated lipid accumulation in dairy GMEC via regulation of ADRP gene. *J Cell Biochem*. 2015;116(1):192–201.
51. Duteil D, Chambon C, Ali F, Malivindi R, Zoll J, Kato S, et al. The transcriptional coregulators TIF2 and SRC-1 regulate energy homeostasis by modulating mitochondrial respiration in skeletal muscles. *Cell Metab*. 2010;12(5):496–508.
52. Yamamuro T, Nakamura S, Yanagawa K, Tokumura A, Kawabata T, Fukuhara A, et al. Loss of RUBCN/rubicon in adipocytes mediates the upregulation of autophagy to promote the fasting response. *Autophagy*. 2022;18(11):2686–96.
53. Kong Y, Zhao C, Tan P, Liu S, Huang Y, Zeng F, et al. FGF21 reduces lipid accumulation in bovine hepatocytes by enhancing lipid oxidation and reducing lipogenesis via AMPK signaling. *Anim (Basel)*. 2022;12(7):939.
54. Capece A, Vasieva O, Meher S, Alfirevic Z, Alfirevic A. Pathway analysis of genetic factors associated with spontaneous preterm birth and pre-labor preterm rupture of membranes. *PLoS ONE*. 2014;9(9):e108578.
55. Sandoval C, Lambo CA, Beason K, Dunlap KA, Satterfield MC. Effect of maternal nutrient restriction on skeletal muscle mass and associated molecular pathways in SGA and Non-SGA sheep fetuses. *Domest Anim Endocrinol*. 2020;72:106443.
56. de Winter TJJ, Nusse R. Running against the wnt: how Wnt/beta-Catenin suppresses adipogenesis. *Front Cell Dev Biol*. 2021;9:627429.
57. Wang L, Xie Y, Chen W, Zhang Y, Zeng Y. miR-34a regulates lipid droplet deposition in 3T3-L1 and C2C12 cells by targeting LEF1. *Cells-Basel*. 2022;12(1):167.
58. Zhao C, Wang Y, Peng Z, Sun X, Sun G, Yuan X, et al. Subacute ruminal acidosis suppressed the expression of MCT1 in rumen of cows. *J Cell Physiol*. 2019;234(7):11734–45.

### Publisher's Note

Springer Nature remains neutral with regard to jurisdictional claims in published maps and institutional affiliations.